About the importance of X-ray elastic constant determination in the precise measurement of residual stress profiles

D. Delbergue [a,b], M. Lévesque [b], P.Bocher [a]
[a] Ecole de technologie supérieur (ÉTS), Canada, dorian.delbergue.1@ens.etsmtl.ca, philippe.bocher@etsmtl.ca;
[b] École Polytechnique de Montréal, Canada, martin.levesque@polymtl.ca

Keywords: Shot peening, Residual stress, X-ray diffraction, X-ray elastic constant, IN718

Introduction

Shot peening is a surface treatment widely used in the aerospace industry in order to improve the fatigue performance of manufactured parts by introducing compressive residual stress at their surface. The residual stresses are actually found in a shallow depth under the surface, delaying both crack initiation and propagation [1]. Thus, accessing the in-depth residual stress profiles with accuracy is essential to calibrate the simulations of the shot peening process [2] or for adequate fatigue life predictions of the components [3]. Any error would lead to the improper calibration of the models.

A large number of techniques can be used for residual stress measurement [4], but not all can quantify the stress gradient introduced by the peening process. X rays having a penetration of few micrometers in metals [5], X-ray diffraction (XRD) techniques are highly suitable for the measurement of residual stress gradients. Consequently, this technique is widely used in industries and laboratories in this regard.

With XRD technique, the residual stress is determined from the measurement of the interplanar spacing through the use of X-ray Elastic Constants (XEC) [6]. They are generally extracted from the literature. Some are determined from single crystal specimens; others are extrapolated from known macroscopic values (Young's modulus and Poisson's ratio) resulting in possible artefacts as demonstrated by the present paper. The stress tensor being measured at the surface of the specimen, the stress in the irradiated layer is biaxial; therefore, only one XEC is required (equivalent to the $\frac{1}{2}S_2=(1+\nu)/E$ in the stress tensor) [6]. As the stress measured by XRD is a linear function of the XEC, any error in the assessment of the $\frac{1}{2}S_2$ value will lead to a proportional error on the measured stress value.

The XEC can be determined following the procedure described in [7,8] as the proportionality constant between the XRD measured stresses versus the known applied stresses. As shown before, even when a non-textured polycrystalline material is used, the determined elastic constants are somewhat different from one XRD measurement method to another [7]. The present work highlights the consequences on the assessment of the residual stress profiles in shot peened Inconel 718 samples using two methods for the calculation of the residual stress: the $\sin^2 \Psi$ and the $\cos \alpha$ methods.

Objectives

The main objectives of this article are to highlight the importance of determining experimentally the XEC for the investigated material and that the constant depends on the diffractometer technique used to determine the residual stresses, introduced in our case by shot peening.

Methodology

In the present work, the XEC for {311} planes were determined with two XRD apparatus for a nickel based superalloy Inconel 718 (IN718); an alloy commonly used in gas turbine engines. The in-depth residual stress profiles of shot peened samples were evaluated over 300 µm using the measured XEC. The microstructure of the material can be described as a bimodal microstructure: One with an average grain size of 8 µm and one with average grain size of 80 µm and a maximum grain size of 150 µm. The last group represents only 0.5% of the grains population but covers 22% of the surface area on which the measurement is performed.

Following the ASTM standard E1426 [9] and the procedure described in [7], the XEC was determined on one flat specimen by uniaxial testing using a 5 kN micro tensile machine from Kammrath & Weiss GmbH. The specimen was carefully prepared by grinding using SiC papers (up to grade 1200) and then electropolished in order to remove potential remaining residual stresses and work hardening. 9 predetermined loads, from 0% up to 70% of the material yield strength (1189 MPa), were used. The known applied tensile stresses were measured via two different types of diffractometers using different methods. The first one varies the β angle (see Fig. 1 for angles definition) and is called the $\sin^2 \Psi$ method. The diffraction peaks are measured on the two linear detectors of a Proto iXRD equipment. The second method uses the α angles to access the values of strain and is called the cos α method. In the later method, a 2D detector measures the full Debye ring of the diffracting grains in one step using a Pulstec µ-X360n equipment. Equations (1) and (2) allow determining the stress for the $\sin^2 \Psi$ method and the cos α method, respectively:

$$\sigma_\varphi = \frac{1}{\frac{1}{2}S_2} \frac{\partial \varepsilon_{\varphi\psi}}{\partial \sin^2 \psi} \tag{1}$$

$$\sigma_\varphi = \frac{1}{\frac{1}{2}S_2} \frac{1}{\sin 2\eta \sin 2\beta} \frac{\partial \overline{\varepsilon}_\alpha}{\partial \cos \alpha} \tag{2}$$

where σ_φ is the surface stress measured along the $\vec{\sigma}_\varphi$ direction, $\frac{1}{2}S_2$ is the elastic constant, $\varepsilon_{\varphi\psi}$ is the measured strain, and $\overline{\varepsilon}_\alpha$ is a parameter calculated from the strain measured at different α angles on the 2D detector, as shown in Fig. 1. The XRD conditions for both apparatus are listed in Table 1. As a first attempt, the XEC was calculated with the macroscopic values of Young's modulus (205 GPa) and Poisson's ratio (0.3) giving $\frac{1}{2}S_{2\,macro.}$ = 6.33E^{-6} MPa^{-1}.

The samples used to illustrate the importance of measuring properly the XEC were two IN718 samples having dimensions of 76.2 mm∗50.8 mm∗10.2 mm made of the same batch of material. They were shot peened with cut wire CW14 at 4A and 8A Almen intensities for 100% coverage. Shot peening was carried out with an air-pressurized shot peening machine manufactured by Canablast and Genik. The in-depth residual stresses were measured by coupling the X-ray diffraction techniques with an electropolishing removal process (electropolishing does not induce additional residual stresses and was done using a perchloric acid-based solution). The reached depths were measured using a Mitutoyo SJ-400 profilometer for better precision. In order to account for stress redistribution caused by the layer removal process, the analytical Moore and Evans correction [10] was applied (as the geometry of the sample and the electropolishing pocket respect the related hypothesis).

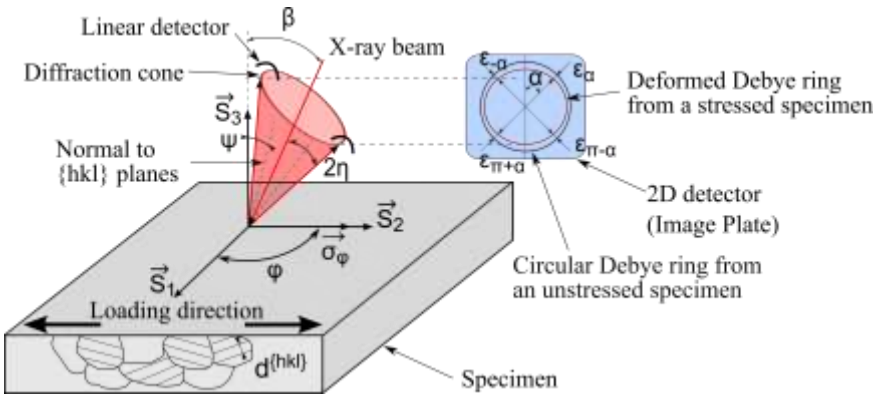

Figure 1: Presentation of diffraction cone and types of detectors.

Table1: XRD conditions

Condition	Proto iXRD	Pulstec μ-X360n
Detectors	2 linear	1 Image Plate
Tube	Mn Kα (λ = 2.103 Å)	Cr Kβ (λ = 2.085 Å)
Diffraction plane, Bragg angle	{311} , 2θ = 151.8°	{311} , 2θ = 148.2°
Number of β inclinations	7 (-28° ≤ Ψ ≤ 28°)	1 (β = 30°)
$\frac{1}{2}S_{2\ macro.}$	$6.33E^{-6}$ MPa^{-1}	

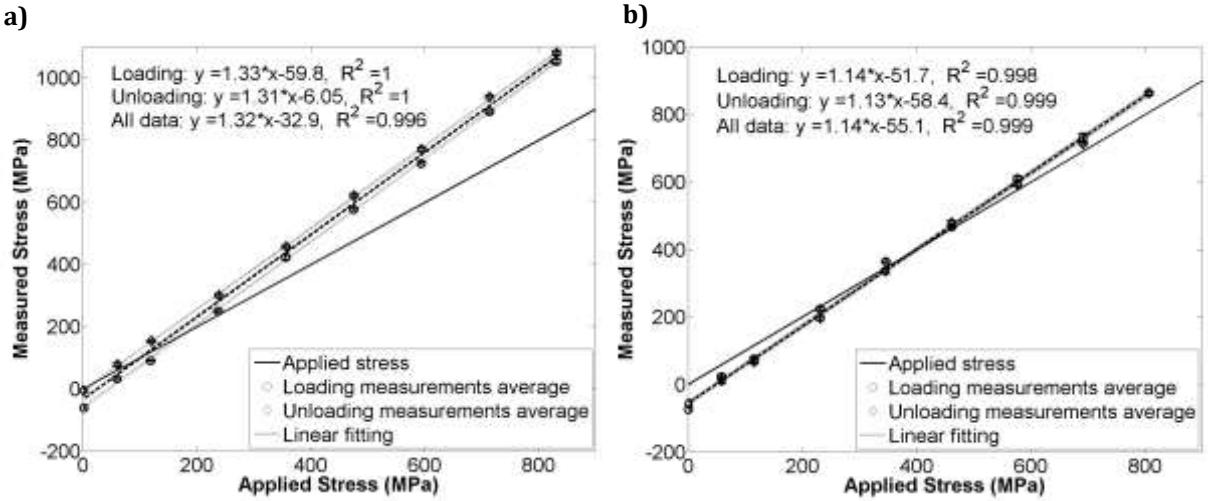

Figure 2: Stresses measured by XRD, calculated with a) the $\sin^2 \Psi$ method (via Proto iXRD) and b) the cos α method (via Pulstec μ-X360n), for different applied tensile stresses.

Results and analysis

The configurations of the two diffractometers and the geometry of the micro-tensile machine didn't allow irradiating the exact same zone of the specimen during tensile tests. Nonetheless, the aperture size was kept the same on the two apparatus so the irradiated volume was similar. It is worth noting that for the Proto apparatus the irradiated volume varies in accordance with the different incident

angles. Fig. 2 presents the average measured stresses versus the applied tensile stresses for the two stress calculation methods. For each measurement, the XRD measurement was repeated 7 times during loading and unloading of the specimen, corresponding respectively to circle markers and diamond markers on the graph. The straight solid line represents the reference line for a hypothetical case where the specimen does not show any residual stress (start from 0 MPa) and where the XEC value would be the one obtained with the macroscopic elastic values of the material. The fitting of loading and unloading measurements is shown by the dotted lines, as well as the global fitting represented by the dashed lines. For each loading, the applied stress was stable enough throughout the measurement duration (about 5 min for the $\sin^2 \Psi$ method and 2 min for the cos α method) to allow the 7 XRD measurements (less than 3 MPa variation was reported). The error bars from the 7 measurements are also plotted and correspond to a 95% confidence interval calculated with the Student's law. The standard deviation of the XRD measurements being less than 25 MPa for most of the loading conditions, the error bars are barely visible for both apparatus. Good measurement repeatability was found for the two apparatus at a given loading condition.
As depicted in Fig. 2 a) & b), the real specimen presents residual stresses at the surface despite the cautious surface preparation: For 0 MPa applied stress, the first combination of apparatus and stress calculation method gives compressive residual stress of -33 MPa (Fig. 2. a)), and the other -55 MPa (Fig. 2 b)). The surface residual stresses are reflected by y-intercepts different than 0 in the linear fittings. However it does not affect the XEC measurement as it is determined via the proportionality constant.
In Fig. 2, the various plots are not parallel to the reference line. The proportionality constants being significantly greater than 1 shows that the use of the XEC obtained from the macroscopic elastic constants of the material introduces significant errors. The total measurement time for the Pulstec was only 6h while 13h for the Proto apparatus, thus the experiment had to be done over two days for this apparatus. Consequently, the point at 70% of the yield strength (800 MPa) has been measured twice: Once as a finishing point for the loading condition (the first day) and once as a starting point for the unloading condition (the second day), as shown in Fig. 2. a). It provides two values having a 30 MPa difference. The loading and unloading fittings are not superimposed showing that the difference in measurements holds between loading and unloading conditions. The difference does not exist for measurements with the Pulstec μ-X360n (Fig. 2. b)). In both cases, the measured stresses are overestimated by 32% and 14%, respectively for the $\sin^2 \Psi$ method and for the cos α method, resulting in corrected XEC values: $\frac{1}{2}S_{2\,\sin^2\psi} = 8.37E^{-6}$ MPa^{-1} and $\frac{1}{2}S_{2\,\cos\alpha} = 7.21E^{-6}$ MPa^{-1}, for the $\sin^2 \Psi$ and cos α methods respectively. In the present case a 15% difference between the two XEC is found, which is more significant than in [7].

Residual stress profiles were then measured for two samples shot peened with CW14 at 4A and 8A Almen intensities. In the present study the measurements were repeated 3 times and averaged. Fig. 3 presents the in-depth profiles for the two shot peening conditions. The stresses are determined with the macroscopic and corrected XEC values. The residual stress profiles show the expected behaviors of shot peening samples: Compressive residual stress is found at the surface, reaching a maximum below the surface and presence of a tensile stress peak participating to the stress balance.

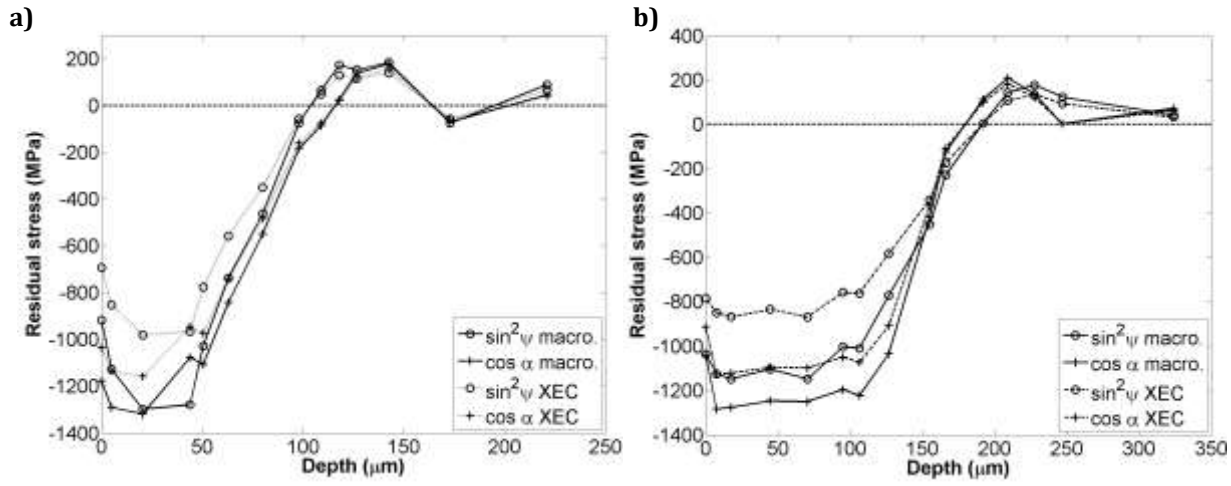

Figure 3: In-depth residual stress profiles for samples shot peened at: a) 4A and b) 8A intensities, measured with the sin² Ψ method (circle symbols) and the cos α method (plus sign symbols), and calculated with macroscopic values and corrected XEC.

The stresses calculated with the macroscopic constants, i.e. $\frac{1}{2}S_{2macro.}$, are linked together by straight lines and are shown in Fig. 3 whereas the stresses corrected with the XEC experimentally determined are linked by dotted lines for the 4A intensity (Fig. 3 a)) and by dashed lines for the 8A intensity (Fig.3 b)). Errors inherent to the calculation method are not shown on the graphs for more clearness, but average error on stress calculation for the sin² Ψ method is typically 50 MPa and the double is found for the cos α method. The use of Kβ rays can explain the higher average error for the last method as they produce lower peak intensity. Nevertheless, the standard deviation of the 3 repeated measurements is higher for the measurements made by the linear detectors than for the 2D detector. Overall, the high errors can also be explained by the shape of the electropolished pocket which is not perfectly flat. In fact, the irradiated zone may have a gradient of depth, combined with the stress gradient, it increases the measurement errors.
For the measurements using the macroscopically determined XEC value, the two stress measurement methods give different surface residual stress values for the 4A sample (Fig. 3 a)); this difference is even more pronounced when the corrected XEC are used. A similar trend is observed for the 8A sample (Fig. 3 b)). A similar maximum compressive stress is found for the 4A sample between the two X-ray methods, while a significant difference in maximum compressive stress is found for the 8A profiles.

Fig. 4 summarizes the corrected profiles. A peak of maximum compressive stress is found for the 4A sample, while a 100 μm plateau of maximum compressive residual stresses is found below the surface for the highest shot peening intensity (8A). A difference of 115 MPa is found between the maximum compressive stresses of the 4A and 8A samples when measured with the sin² Ψ method, whereas, the difference is found to be only 30 MPa when measured with the cos α method, making the profiles more coherent as the increase in shot peening intensity is known to increase the depth at which the maximum compressive stress is found. The compressive stresses are then partially balanced by a noticeable tensile peak of about150 MPa to 200 MPa located at 143 μm below the surface for the 4A sample. For the 8A sample, the tensile peak is found at a depth of 230 μm when measured with the Proto and at 210 μm when measured with the Pulstec.

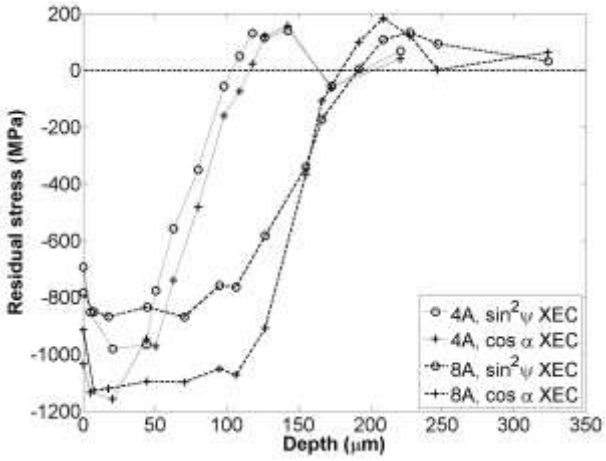

Figure 4: Presentation of the corrected in-depth residual stress profiles for the 4A and 8A samples.

Residual stress profiles may be used for the finite element calibration of shot peening process simulations, or for prediction of fatigue life when use as model input. Therefore, they must accurately describe the real residual stress state.

Conclusions

X-ray Elastic Constants measured with two different X-ray diffraction methods were found to differ significantly from the one calculated with macroscopic constants and from one XRD technique to the next, even if they are measured on the same family of plane. The use of macroscopic values would have introduced an error of about 32% to 14%, depending on the method used in these conditions. The corrections were applied on residual stress profiles measured on shot peened Inconel 718 samples and significant differences were found between the two stress calculation methods. Finally, the measured 4A and 8A profiles are more coherent when measured with the cos α method and the 2D detector than with the $\sin^2 \Psi$ method and the linear detectors.

Acknowledgement

This work was financially supported by CRIAQ, NSERC, Mitacs, Pratt & Whitney Canada, Bell Helicopter Textron Canada, L3-Communications MAS and Heroux-Devtek.

References

[1] E.R. De Los Rios, A. Walley, M.T. Milan, G. Hammersley, Fatigue crack initiation and propagation on shot-peened surfaces in A316 stainless steel, Int. J. Fatigue. 17 (1995) 493–499. doi:10.1016/0142-1123(95)00044-T.

[2] F. Tu, D. Delbergue, H.Y. Miao, T. Klotz, M. Brochu, P. Bocher, M. Lévesque, A sequential DEM-FEM coupling method for shot peening simulation, Surf. Coat. Technol. 319 (2017) 200–212. doi:10.1016/j.surfcoat.2017.03.035.

[3] T. Klotz, D. Delbergue, H.Y. Miao, A. Castro-Moreno, P. Bocher, M. Lévesque, M. Brochu, Analytical fatigue life prediction of shot peened Inconel 718, in: Int. Conf. Shot Peen., Montreal, Canada, 2017.

[4] G.S. Schajer, Practical Residual Stress Measurement Methods, Wiley, 2013.

[5] B.D. Cullity, Elements of X-ray diffraction, Addison-Wesley Publishing Company, Inc., 1956.

[6] I.C. Noyan, J.B. Cohen, Residual stress measurement by diffraction and interpretation, Springer-Verlag, New York, 1987.

[7] D. Delbergue, D. Texier, M. Lévesque, P. Bocher, Comparison of Two X-Ray Residual Stress

Measurement Methods : Sin 2 ψ and Cos α, Through the Determination of a Martensitic Steel X-Ray Elastic Constant, in: T.M. Holden, O. Muránsky, L. Edwards (Eds.), Intern. Conf. Residual Stress. 2016, Sydney, Australia, 2016: pp. 55–60. doi:10.21741/9781945291173-10.

[8] A.S.M.Y. Munsi, A.J. Waddell, C.A. Walker, A Method for Determining X-ray Elastic Constants for the Measurement of Residual Stress, Strain. 39 (2003) 3–10. doi:10.1046/j.1475-1305.2003.00044.x.

[9] ASTM, E1426-98 Standard Test Method for Determining the Effective Elastic Parameter for X-Ray Diffraction Measurements of Residual Stress, (2009). doi:10.1520/E1426-98R09E01.

[10] M.G. Moore, W.P. Evans, Mathematical correction for stress in removed layers in X-ray diffraction residual stress analysis, SAE Trans. 66 (1958) 340–345. doi:10.4271/580035.